Electronic supplementary information

Oxygen-vacancy-containing Nb_2O_5 nanorods with modified semiconductor character for boosting selective nitrates-to-ammonia electroreduction

Bo Cao, [a,b] Xun Xu, [a,b*] Zhuozheng Hong, [a,b] Junzhi Liao, [a,b] Ping Li, [a,b] Hao Zhang, [a,b] and Shuwang Duo, [a,b*]

[a] *School of Materials and Mechanical & Electrical Engineering, Jiangxi Science and Technology Normal University, Nanchang 330013, China*

[b] *Jiangxi Key Laboratory of Surface Engineering, Jiangxi Science and Technology Normal University, Nanchang, 330013, China Email: rozen121@163.com, swduo@126.com*

1. Experimental details

1.1 Chemicals

All chemicals were analytical grade and used as received without further purification. The chemicals were purchased from Aladdin Chemical reagent Co., Ltd. (Shanghai, China). Deionized (DI) water was used in all experiments

1.2 Instrumentation

The morphologies of the samples were characterized by scanning electronic microscopy (SEM) using a microscope (FEI, Tecnai G220 S-TWIN,US) and transmission electron microscope (TEM) using a microscope (JEOL Ltd. JEM-2100f, Japan).X-ray diffraction (XRD) of all the prepared materials were performed on diffraction instrument (Sinmadzu, XRD-6100, Japan). Spectrophotometry vis UV/Vis spectrophotometer (UV-1800 S). X-ray photoelectron spectroscopy (XPS, Thermo Scientific, K-Alpha ,US) was used to analyze the chemical state of the oxide. Ion chromatograph was used to detect and analyze ions in solution (Aquion ICS-1100).

1.3 Ion concentration detection methods

The ion concentration of the electrolyte diluted to a suitable concentration was measured with a UV-Vis spectrophotometer and Ion chromatography to match the range of the calibration curve.Specific detection methods are as follows：

1.3.1 UV-Vis spectrophotometer

Detection of nitrate-N: Firstly, 2.0 mL electrolyte was taken out from the electrolytic cell and diluted to 5 mL to detection range. Then, 0.1 mL 1 M HCl and 0.01 mL 0.8 wt% sulfamic acid solution were added into the aforementioned solution. After 15 minutes, the absorbance was detected by UV-Vis spectrophotometry at a wavelength of 220 nm and 275 nm. The final absorbance of nitrate-N was calculated based on the following equation: $A=A_{220}nm -2A_{275}nm$. The correction curve can be obtained by $NaNO_3$ solution of different concentrations and corresponding absorbance.

Detection of ammonium-N: With 4.1667 g of sodium hydroxide, 5 g of salicylic acid and 5 g of sodium citrate, 100mL solution A was prepared .9.0 mL sodium hypochlorite solution was prepared into 100 mL solution B. 1 g sodium ammonium ferricyanide (C5FeN6Na2O) in 100 mL solution C. 2ml of electrolyte was taken out

of the electrolytic cell, and then 1ml of liquid A, 1ml of liquid B and 0.5ml of liquid C were respectively taken to prepare A 5ml mixed solution After shaking and standing for 1 h , the absorbance was tested by UV-Vis spectrophotometry at a wavelength of 655 nm. The calibration curve can be obtained through different concentrations of NH_4Cl solutions and the corresponding absorbance.

1.3.2 Ion chromatography

Detection of ammonium-N and nitrate-N: After pretreatment, the samples were determined according to the set chromatographic conditions, using external standard method Quantification, the response value of ammonium ion in the sample solution to be measured should be within the linear range of the standard curve Chromatographic peak retention time should be consistent with the standard substance

1.4 Electrochemical measurements

Electrochemical measurements were performed using an electrochemical workstation (Princeton, VersaSTAT 4, US) by employing an air-proof two-compartment cell separated by a Nafion membrane. The working, counter, and reference electrodes were sample foil, silver chloride electrode, and platinum foil, respectively. The working electrode was cut into a small square with a surface area of 1 cm × 1 cm. A 0.5 M Na_2SO_4 aqueous solution with $NaNO_3$ (50 ppm nitrate-N) was used as both the catholyte (35 mL) and anolyte (35 mL). Ar (99.995 vol%) gas was continuously fed into the solution throughout the tests (see Supporting Information for details). All the potentials were recorded on an RHE and all the polarisation curves were stable after continuous circulation.

1.5 Calculation of the yield, selectivity, and Faradaic efficiency.

Potentiostatic tests were conducted to measure the yield, selectivity, and Faradaic efficiency of NH_3 and the conversion of NO_3^- The potentiostatic test (0.5 M Na_2SO_4 aqueous solution with $NaNO_3$ 50 ppm nitrate-N) was carried out at different potentials for 2 h with a stirring rate of 300 rpm. The concentration of NH_3 and NO_3^- in

electrolyte was detected at intervals (0, 1, 2 h).

The conversion of NO_3^- was calculated using the Eq. S1:

NO_3^- conversion = $\Delta C_{NO3-} / C_0 \times 100\%$ (Eq. S1)

The selectivity of the product calculated using the Eq. S2:

NH_3 selectivity (S_{NH3})=$C_{NH3}/\Delta C_{NO3-} \times 100\%$ (Eq. S2)

The yield of NH_3 (aq) was calculated using the Eq. S3:

Yield NH_3 = $(C_{NH3} \times V) / (M_{NH3} \times t \times m)$ (Eq. S3)

The Faradaic efficiency was calculated using the Eq. S4:

Faradaic efficiency = $(8F \times C_{NO3-} \times V) / (M_{NO3-} \times Q) \times 100\%$ (Eq. S4)

where C_0 is the initial concentration of NO_3^-, ΔC_{NO3-} is the concentration difference of NO_3^- before and after electrolysis, C_{NH3} is the concentration of NH_3 (aq, t (s) is the electrolysis time, F is the Faradaic constant (96485 C mol^{-1}), V is the electrolyte volume, m is the mass of catalyst, Q is the total charge passing the electrode.

2. Additional Figures and Tables

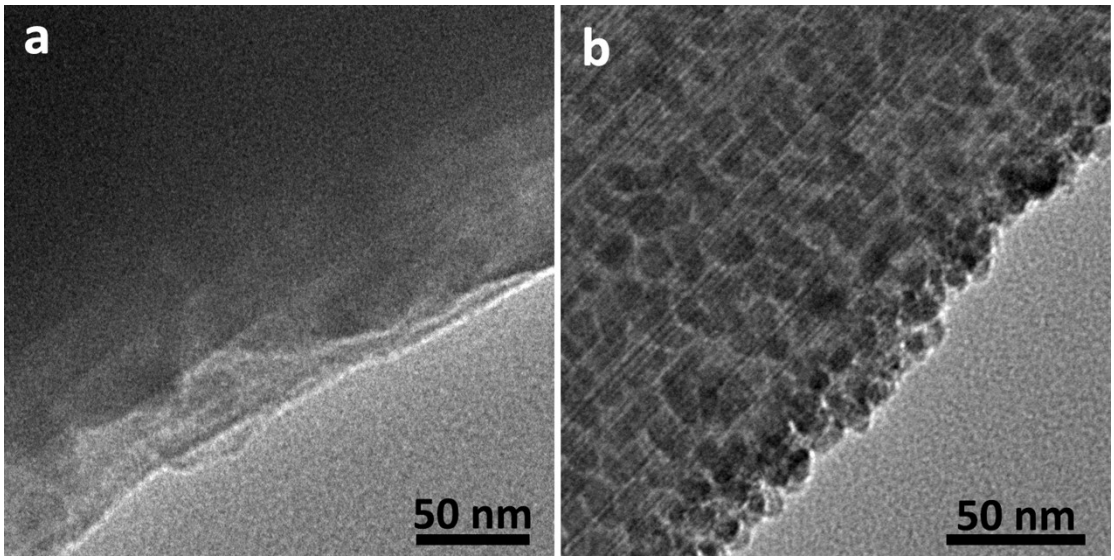

Fig. S1 TEM images of Nb_2O_5 (a) and Nb_2O_{5-x} (b)

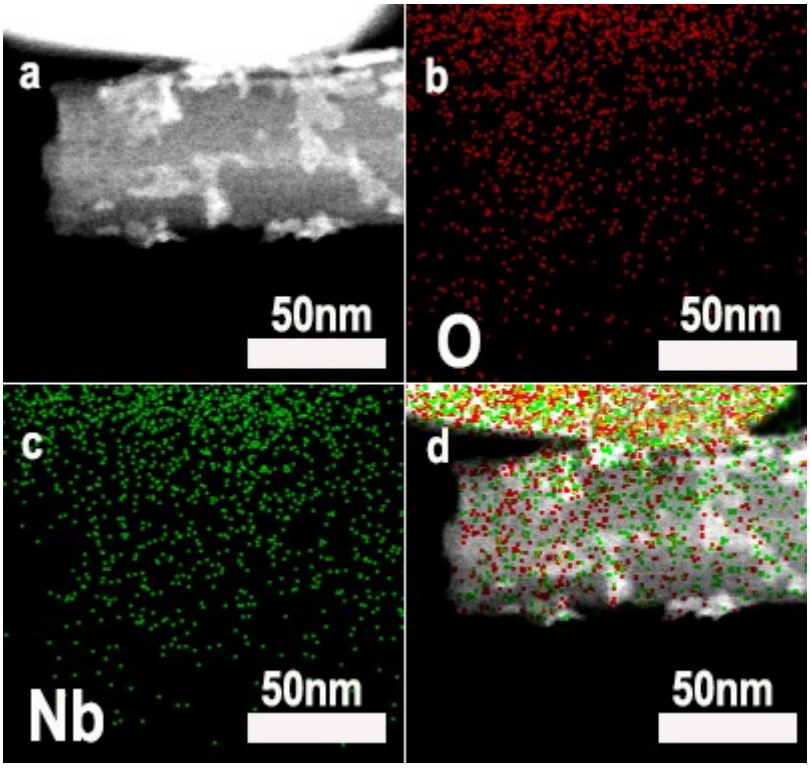

Fig. S2 (a) HAADF-STEM image of Nb_2O_{5-x} together with EDX mapping images of (b) O, (c) Nb, and (d) the total elements distribution

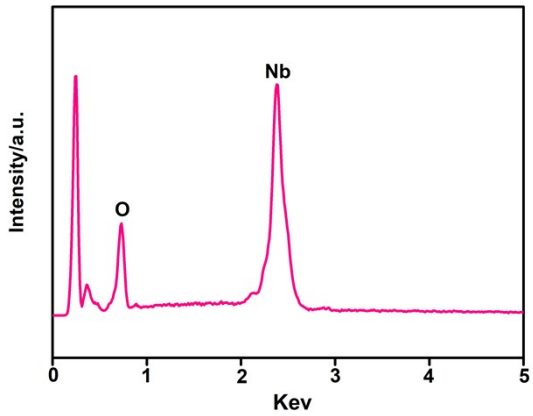

Fig. S3 EDX spectra of Nb_2O_{5-x}

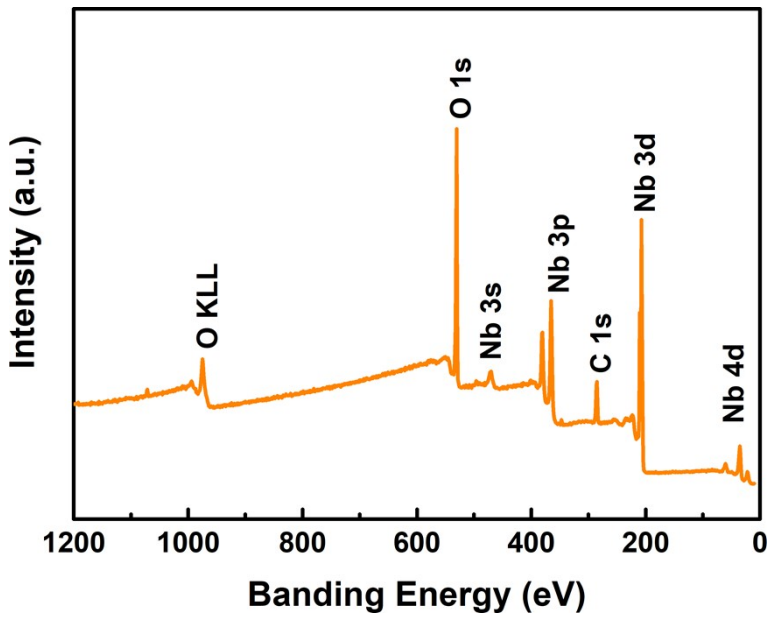

Fig. S4 The Full XPS spectra of Nb_2O_{5-x}

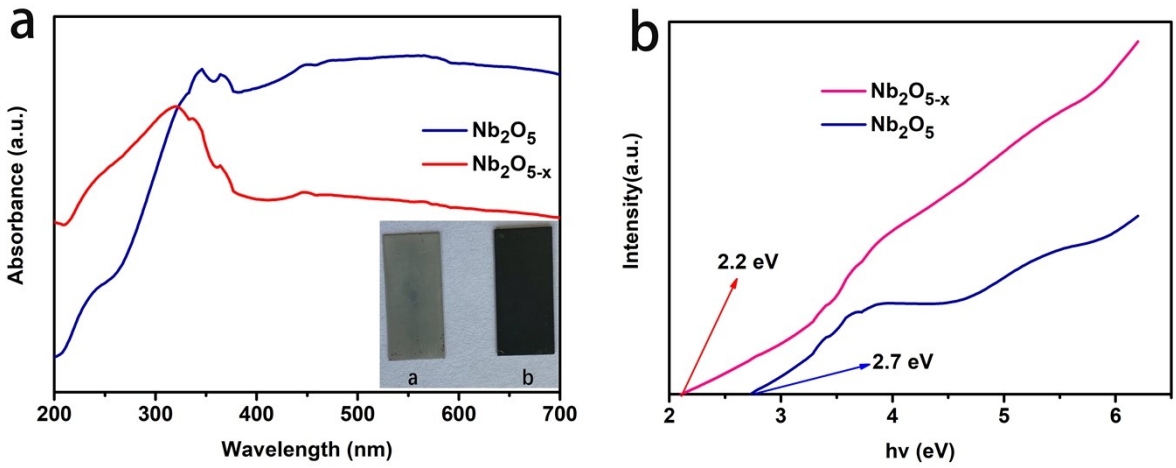

Fig. S5 The Ultraviolet-visible diffuse reflectance spectra (UV-vis DRS) of Nb_2O_{5-x} and Nb_2O_5(a), (b) the Band gap of Nb_2O_{5-x} and Nb_2O_5

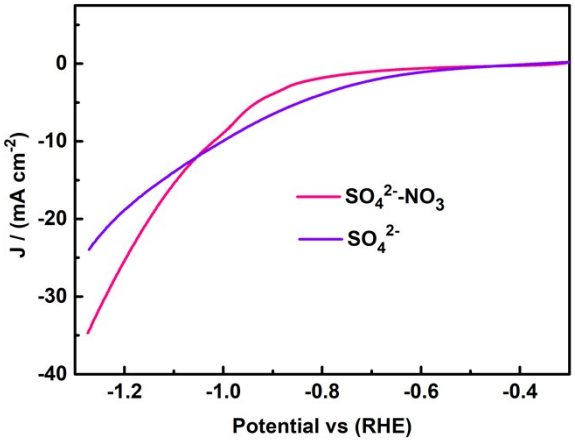

Fig. S6 Linear scan voltammetry curves of Nb_2O_{5-x} with different electrolyte. The larger current in nitrate electrolyte suggests the reaction of nitrate electroreduction.

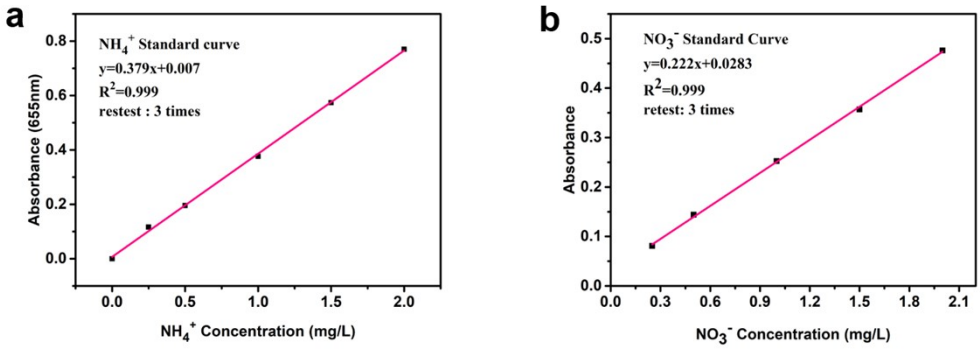

Fig. S7 The UV-Vis absorption spectra and the corresponding calibration curves: (a) NH_4^+-N, (b) NO_3-N, The concentration of nitrate, and ammonia were all referred as nitrogen (NO_3^--N, NH_4^+-N), and the ultrapure water was used as background solution.

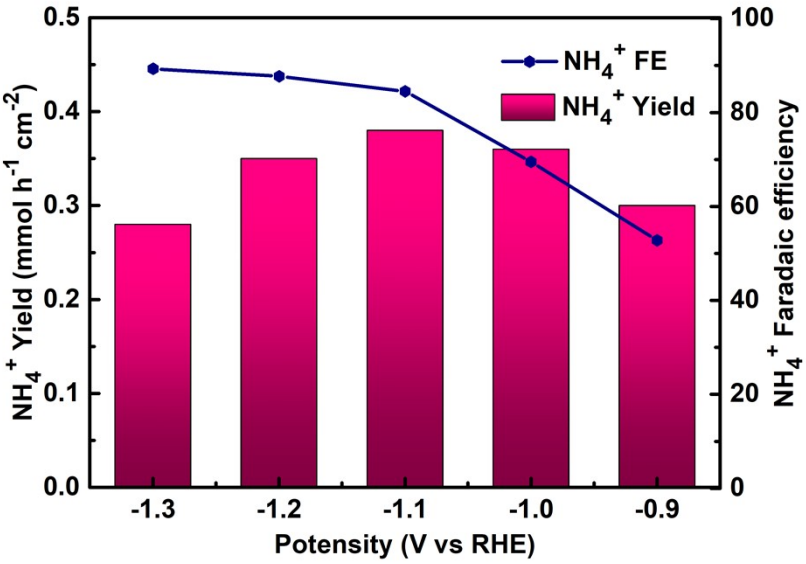

Fig. S8 The faradaic efficiency and yield of ammonium over Nb_2O_{5-x} at different potentials.

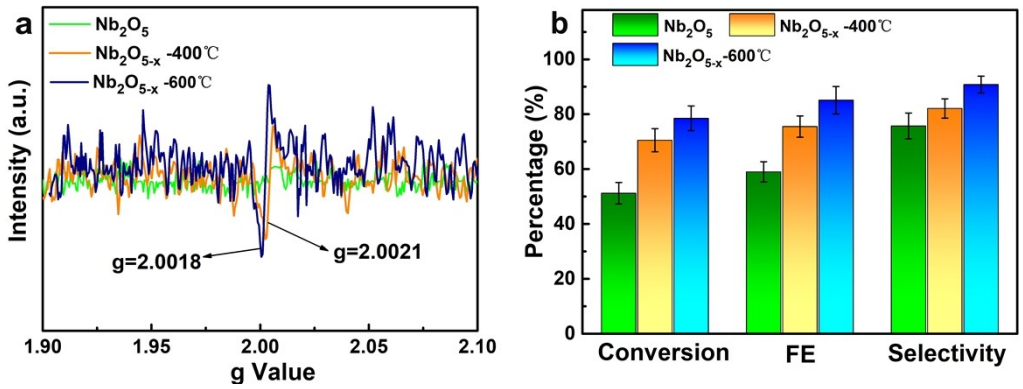

Fig. S9 (a) EPR spectra , (b)ENRA test data of Nb_2O_5 with different thermal condition

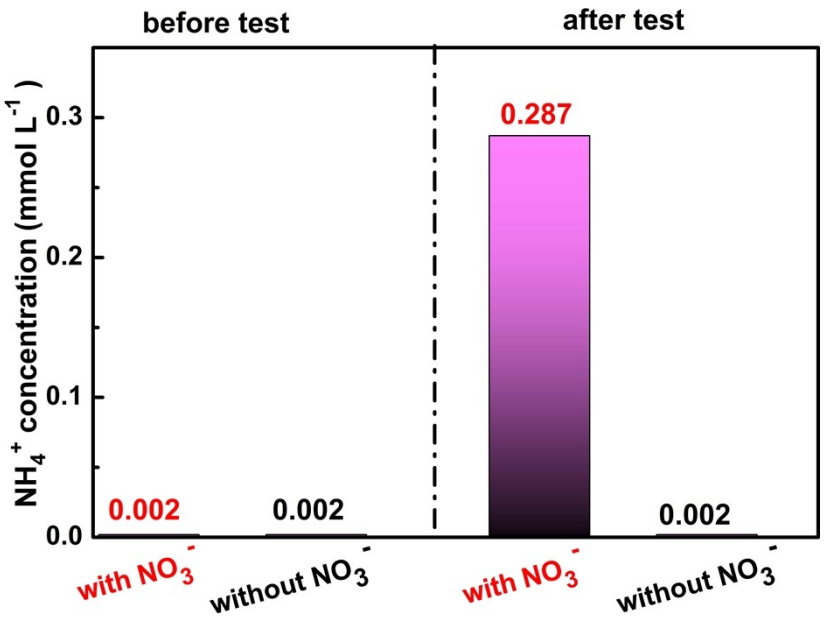

Fig. S10 The ammonia concentration of solution (before and after potentiostatic tests) over Nb_2O_{5-x} in 0.5 M Na_2SO_4 electrolyte with and without NO_3^-.

.

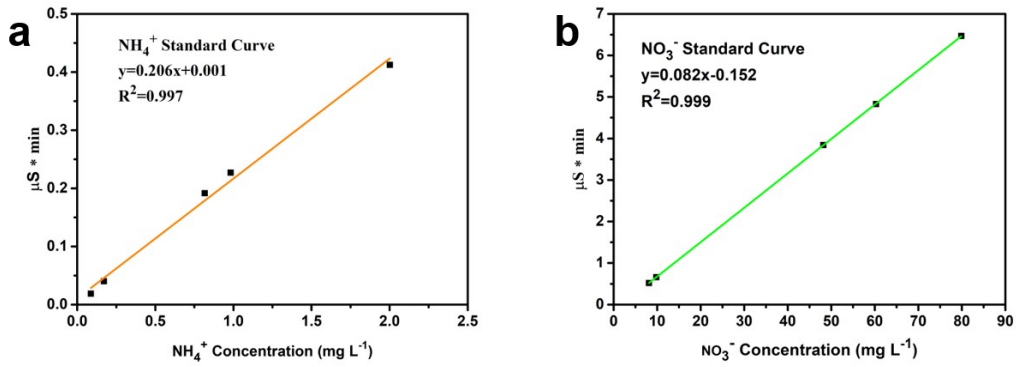

Fig. S11 The ion chromatography absorption spectra and the corresponding calibration curves: (a) NH_4^+-N, (b) NO_3-N.

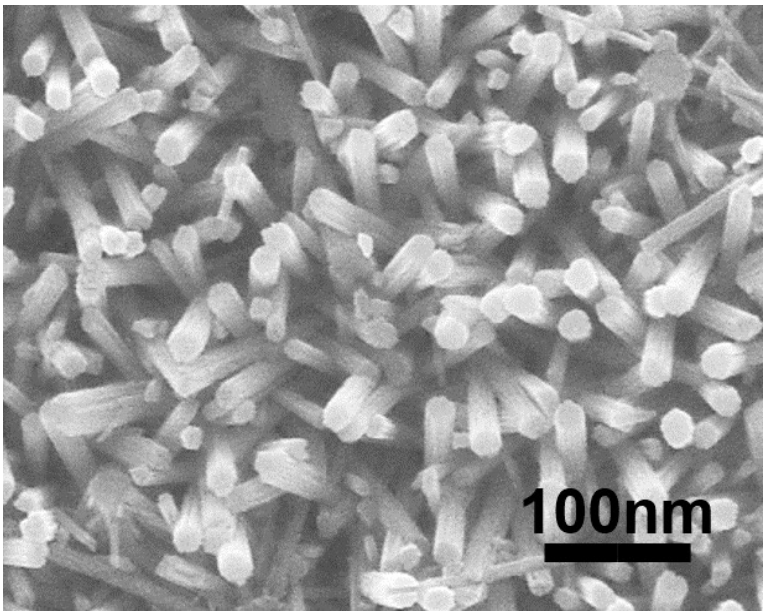

Fig. S12 SEM images of Nb_2O_{5-x} after cycling tests

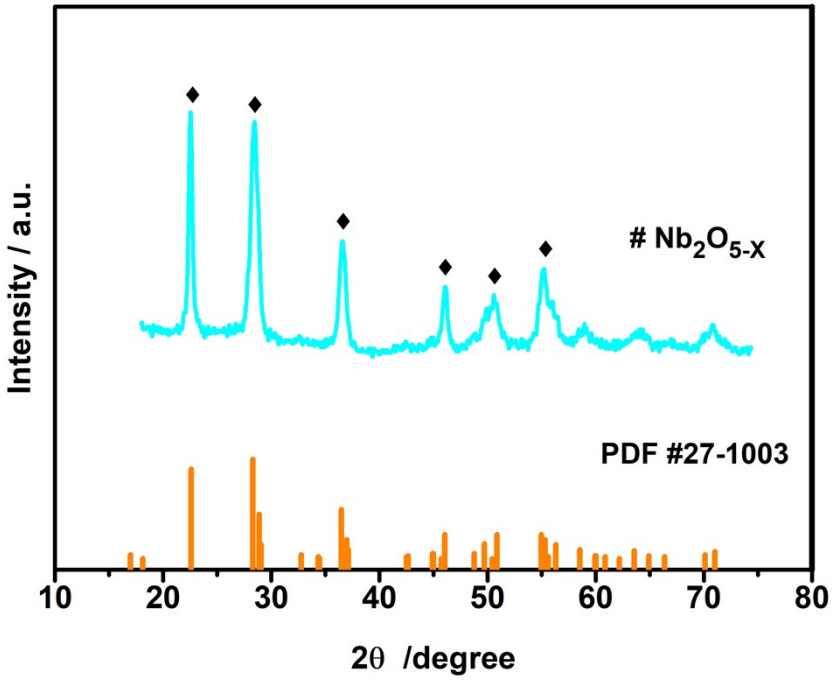

Fig. S13 XRD pattern of Nb_2O_{5-x} after cycling tests

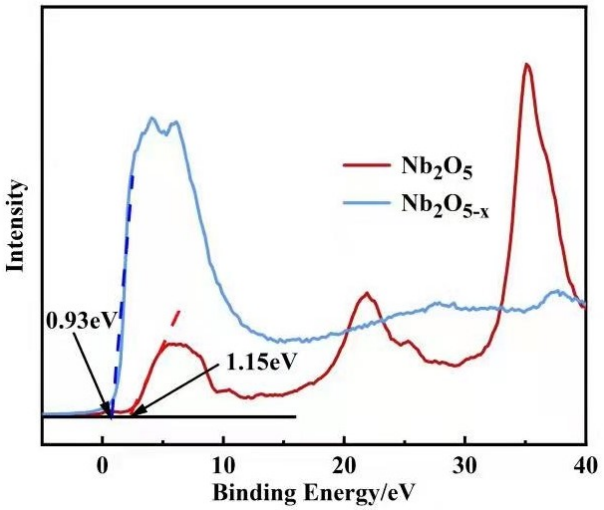

Fig. S14 VB-XPS spectra of Nb_2O_{5-x} and Nb_2O_5

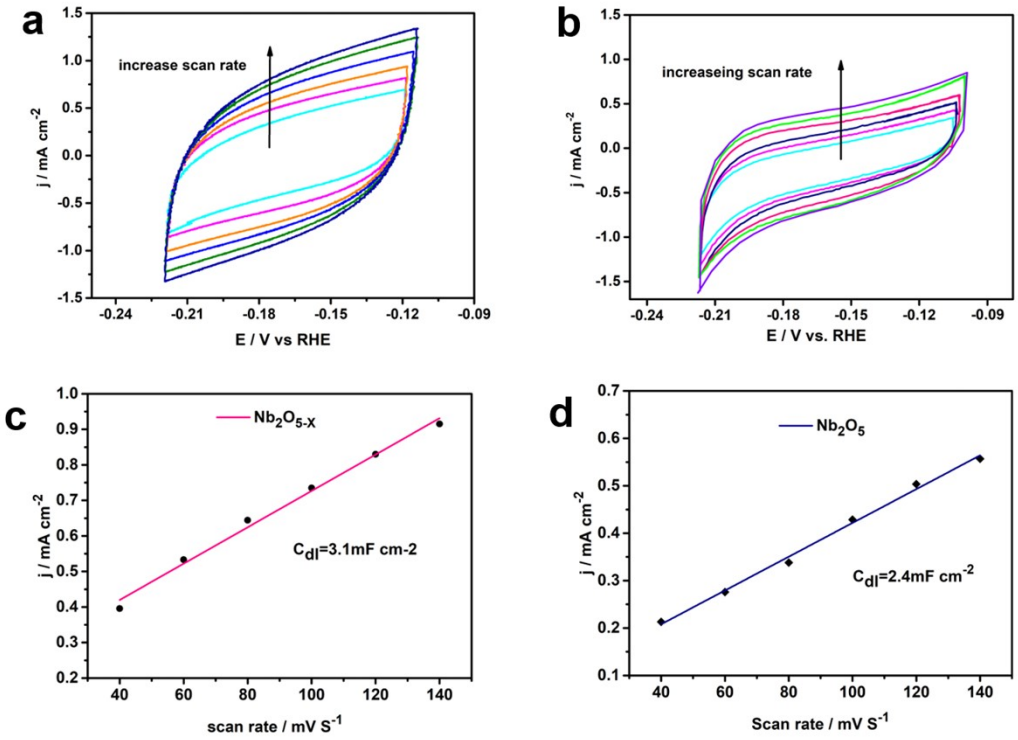

Fig. S15 Cyclic voltammogram curves of Nb_2O_{5-X} (a) and Nb_2O_5 (b) with various scan rates from 60 to 160 mV s^{-1}. The difference in current plotted against scan rate showing the extraction of the double-layer capacitances (c) and (d), which allow the estimation of the electrochemically active surface area (ECSA).

Table S1. Comparison of ammonia selectivity by electrocatalytic nitrate reduction

Electrocatalyst	Electrolyte	Performance	Detecting method	Ref
Nb_2O_{5-x} (This work)	**0.5 M Na_2SO_4 50 ppmNO_3^--N**	**FE (NH_3): 85.1% S (NH_3): 90.8% Y(NH_3) : 287 μmol $h^{-1}cm^{-2}$**	**UV-Vis spectroscopy Ion chromatography**	**This work**
Ni-Fe0@Fe_3O_4	50 ppm NO_3^--N + 10 mM NaCl	S (NH_3):10.4%	UV visible spectrophotometer	[1]
TiO_{2-x} nanotubes	50 mM Na_2SO_4 + 50 ppm NO_3^--N	S (NH_3): 87.1% FE (NH_3):85% Y(NH_3) : 45 μmol $h^{-1}cm^{-2}$	UV-Vis spectroscopy 1H NMR	[2]
Co_3O_4-TiO_2-PVP	IrO_2-RuO_2/Ti ⏐0.1 M Na_2SO_4, $NaNO_3$ (10 mA cm^{-2})	S (NH_3): 73%-	UV-vis spectroscopy	[3]
Co_3O_4/NiO HNTs	0.5 M Na_2SO_4 200 ppmNO_3^--N	FE (NH_3): 55% S (NH_3): 62.3% Y(NH_3) : 6.9 μmol h^{-1} mg_{cat}^{-1}	UV-vis spectroscopy	[4]
PTCDA/O-Cu	0.1 M PBS + 500 ppm NO_3^--N	FE (NH_3): 77±3% Y(NH_3) : 436±85 μg $h^{-1}cm^{-2}$	UV-vis spectroscopy	[5]
Ti/TiHx	0.1 M HNO_3 + 0.3 M KNO_3	FE (NH_3): 82%	UV-vis spectroscopy	[6]
Bi_2O_3-CC	50 M K_2SO_4 + 750 ppm NO_3^--N	FE (NH_3): 84.9% S (NH_3): 80.3%	UV-vis spectroscopy	[7]
CuO nanoplates	50 ppm NO^{3-} + 0.0 M Na_2SO_4	*S* (NH_3): 81.99% Y(NH_3) : 781.25 μg $h^{-1}cm^{-2}$	UV-vis spectroscopy	[8]
3D Cu-Pt bimetallic	50 ppm NO^{3-}+ 0.5 M Na_2SO_4,	*S* (NH_3): 84%	UV-vis spectroscopy	[9]
Pd（110）facts	0.1 M NaOH + 400 ppm NO^{3-}-N	FE (NH_3): 35% Y (NH_3): 306.8 μg h^{-1} mg_{Pd}^{-1}	UV-vis spectroscopy	[10]
Fe single atom	0.50 M KNO_3/0.10 M K_2SO_4 mixed electrolyte	*S* (NH_3): 75% FE (NH_3): 76% Y(NH_3) : 460 μmol $h^{-1}mg_{cat}^{-1}$	1H NMR	[11]

Note:

Y (NH_3): The yield of ammonia;

FE (NH_3): The Faradaic efficiency of ammonia;

S (NH_3): The selectivity of ammonia;

Reference

1. Z. A. Jonoush, A. Rezaee and A. Ghaffarinejad, *J. Cleaner Prod.*, 2020, **242**, 118569.
2. R. Jia, Y. Wang, C. Wang, Y. Ling, Y. Yu and B. Zhang, *ACS Catal.*, 2020, **10**, 3533-3540.
3. J. Gao, B. Jiang, C. Ni, Y. Qi, Y. Zhang, N. Oturan and M. A. Oturan, *"Appl. Catal., B"*, 2019, **254**, 391-402.
4. Y. Wang, C. Liu, B. Zhang and Y. Yu, *Sci. China Mater.*, 2020, **63**, 2530-2538.
5. G.-F. Chen, Y. Yuan, H. Jiang, S.-Y. Ren, L.-X. Ding, L. Ma, T. Wu, J. Lu and H. Wang, *Nat. Energy*, 2020, **5**, 605-613.
6. J. M. McEnaney, S. J. Blair, A. C. Nielander, J. A. Schwalbe, D. M. Koshy, M. Cargnello and T. F. Jaramillo, *ACS Sustainable Chem. Eng.*, 2020, **8**, 2672-2681.
7. M. Chen, J. Bi, X. Huang, T. Wang, Z. Wang and H. Hao, *Chemosphere*, 2021, **278**, 130386.
8. Y. Xu, M. Wang, K. Ren, T. Ren, M. Liu, Z. Wang, X. Li, L. Wang and H. Wang, *J. Mater. Chem. A*, 2021, **9**, 16411-16417.
9. G. A. Cerrón-Calle, A. S. Fajardo, C. M. Sánchez-Sánchez and S. Garcia-Segura, *"Appl. Catal., B"*, 2021, 120844.
10. J. Lim, C.-Y. Liu, J. Park, Y.-H. Liu, T. P. Senftle, S. W. Lee and M. C. Hatzell, *ACS Catal.*, 2021, **11**, 7568-7577.
11. Z.-Y. Wu, M. Karamad, X. Yong, Q. Huang, D. A. Cullen, P. Zhu, C. Xia, Q. Xiao, M. Shakouri and F.-Y. Chen, *Nat. Commun.*, 2021, **12**, 1-10.